Impact of MAI and Channel Estimation Errors on the Performance of Rake Receivers in UWB Communications

Antonio A. D'Amico, Umberto Mengali, *Fellow, IEEE*, and Lorenzo Taponecco

***Abstract*—The performance of Rake receivers for ultrawideband communications is discussed, taking into account the effects of multiple access interference (MAI) and channel estimation errors. Two alternative signaling formats are considered: time-hopping pulse-position modulation (TH-PPM) and TH pulse-amplitude modulation (TH-PAM). The channel exhibits multipath propagation and its impulse response is either assumed known or is estimated with least squares methods. Computer simulations show that, even with perfect channel knowledge (PCK), TH-PAM is superior to TH-PPM. The superiority increases with the number of users and becomes substantial in the presence of channel estimation errors. An intuitive explanation of this fact is provided.**

***Index Terms*—Channel estimation, pulse-amplitude modulation (PAM) and pulse-position modulation (PPM), Rake receivers, ultrawideband (UWB) systems.**

I. Introduction

THE RECENT initiative of the Federal Communication Committee (FCC) to regulate the use of commercial ultrawideband (UWB) radio has spurred intense research activity in industrial and academic institutions [1], [2] in view of the exploitation of the vast unlicensed spectrum from 3.1 to 10.6 GHz. The interest for commercial applications, especially in the area of short-range communications, stems from several attractive features of UWB technology. First, signal echoes with differential delays on the order of nanoseconds can be resolved and combined, thereby exploiting the multipath diversity of the indoor channel [3], [4]. Secondly, multiple access to the channel is guaranteed to many users. Finally, UWB systems operate at very low power spectral densities and, as such, have the potential of overlaying existing narrowband systems with minimal interference.

Multiple access in UWB communications is accomplished with traditional spread-spectrum techniques. Most of the research carried out so far is concerned with time-hopping (TH) spread spectrum, associated with either binary pulse-position modulation (TH-PPM) [1] or bipolar pulse-amplitude modulation (TH-PAM) [5]. A third option consists of replacing TH with direct-sequence (DS) techniques while still using PAM signaling [6]. In the following, we concentrate on TH-PPM and TH-PAM.

The performance of Rake receivers operating with TH-PPM has been investigated in [7] in the absence of multiple access interference (MAI) and assuming perfect channel knowledge (PCK). The impact of MAI on the detection process is discussed in [1] with line-of-sight (LOS) propagation. In the present paper, we extend these results in various ways. Our aim is to compare the performance of Rake receivers operating with either TH-PPM or TH-PAM, taking MAI and channel estimation errors into account. The indoor propagation channel is taken from [8]. Although other statistical models are available (see [8] and [9] and references therein), we believe that our conclusions hold true in general. Channel estimation is performed with the method described in [10], which was originally designed for the TH-PPM but is trivially extended to TH-PAM.

The main question we address is which of TH-PPM and TH-PAM is better in terms of bit error rate (BER). The answer is obvious if there is no MAI, the channel is known, and the intersymbol interference is negligible. In these circumstances, the signals corresponding to "0" and "1" are antipodal with TH-PAM and orthogonal with TH-PPM. Thus, we expect a gain of 3 dB of TH-PAM over TH-PPM. In the presence of MAI, the question is so complex that physical intuition does not help and an analytical approach seems impossible. Clearly, MAI plays a role both in channel estimation and in data detection. Our simulations indicate that the estimation task is crucial and a much better accuracy is achieved with TH-PAM. As a consequence, this modulation is superior in terms of overall receiver performance.

The rest of the paper is organized as follows. Section II recalls the TH-PAM and TH-PPM formats and presents an overview of the channel model. Section III outlines the receiver structure and the channel estimation algorithm. Simulations are discussed in Section IV, and conclusions are drawn in Section V.

II. Signal and Channel Models

A. Signal Model

An information symbol is transmitted by repeating a short pulse $g(t)$ (referred to as monocycle) over N_f frames, each of duration T_f. As is done in many theoretical studies, we take $g(t)$ as the second derivative of a Gaussian function with a

Manuscript received September 5, 2003; revised July 15, 2004, August 2, 2004 and October 2, 2004; accepted October 10, 2004. The editor coordinating the review of this paper and approving it for publication is L.-C. Wang.

The authors are with the Department of Information Engineering, University of Pisa, 56100 Pisa, Italy (e-mail: antonio.damico@iet.unipi.it; umberto.mengali@iet.unipi.it).

Digital Object Identifier 10.1109/TWC.2005.853918

support $[0, T_g]$ on the order of a nanosecond. The duty cycle T_f/T_g is very large, say a hundred or more. With the TH-PPM format, the transmitted signal is represented by

$$s(t) = \sum_i b(t - iN_fT_f - a_i\Delta) \tag{1}$$

with

$$b(t) = \sum_{j=0}^{N_f-1} g(t - jT_f - c_jT_c). \tag{2}$$

The PPM modulation is revealed in (1) by the time shifts $a_i\Delta$, where a_i are binary (0 or 1) data and the time parameter Δ is comparable in size with T_g. It has been shown [1] that its choice affects the detection process and can be exploited to optimize the system performance on LOS channels. In the following, we set Δ equal to $2T_g$, which makes the waveforms $b(t)$ and $b(t-\Delta)$ orthogonal. The parameter T_c is the chip duration and the sequence $\{c_j\}$ is the user's time-hopping code, with elements taking integer values in the range $0 \le c_j \le N_h - 1$. As is known, time hopping accomplishes two tasks: it provides multiple access capability and smoothes out the spectral lines caused by the repetition pattern [11].

With the TH-PAM format, (2) remains unchanged while (1) becomes

$$s(t) = \sum_i a_i b(t - iN_fT_f) \tag{3}$$

where the data a_i belong to the alphabet ± 1. Whatever the signaling format, in the sequel, the data symbols are modeled as independent identically distributed (i.i.d.) random variables.

B. Channel Model

The signal propagates through a multipath channel and its echoes arrive in clusters. The channel impulse response has the form [8]

$$h(t) = X \sum_{l=1}^{L} \sum_{k=1}^{K} \alpha_{k,l}\delta(t - T_l - \tau_{k,l}) \tag{4}$$

where X reflects the attenuation due to shadowing, $\alpha_{k,l}$ is the gain coefficient of the kth ray in the lth cluster, T_l is the arrival time of the lth cluster, and $\tau_{k,l}$ is the delay of the kth ray in the lth cluster relative to the beginning of the cluster. Cluster arrival times are Poisson distributed with rate Λ and rays within a cluster also arrive according to a Poisson law with rate λ. The shadowing factor X has a log-normal distribution, i.e., $20\log_{10} X \in \mathcal{N}(0, \sigma_x^2)$. Similarly, the gain coefficients fade independently of each other and are log-normally distributed, i.e.

$$20\log_{10}\alpha_{k,l} \in N\left(\mu_{k,l}, \sigma_1^2 + \sigma_2^2\right) \tag{5}$$

where $\mu_{k,l}$, which reflects the power decay over the clusters and within a given cluster, is given by

$$\mu_{k,l} = \frac{10\ln\Omega_0 - \frac{10T_l}{\Gamma} - \frac{10\tau_{k,l}}{\gamma}}{\ln 10} - \frac{\left(\sigma_1^2 + \sigma_2^2\right)\ln 10}{20}. \tag{6}$$

In this equation, Γ and γ are the cluster decay factor and the ray decay factor, respectively, whereas Ω_0 is the mean energy of the first ray in the first cluster.

In the simulations discussed later, Ω_0 is chosen so as to normalize to unity the total energy in the gains $\{\alpha_{k,l}\}$. This is easily accomplished bearing in mind that the expectation of $\alpha_{k,l}^2$ equals $\Omega_0 \mathrm{e}^{-T_l/\Gamma}\mathrm{e}^{-\tau_{k,l}/\gamma}$. The following parameter values have been chosen: $\Lambda = 0.0667$ ns^{-1}, $\lambda = 2.1$ ns^{-1}, $\Gamma = 14.00$, $\gamma = 7.9$, $\sigma_1 = \sigma_2 = 3.39$ (dB), and $\sigma_x = 3$ (dB). They correspond to a 4–10-m channel with non-LOS propagation [8] and a maximum delay spread of about 60–70 ns.

C. Received Waveform

It is assumed that K_u users are simultaneously active in the environment. All of them adopt the same signaling format (either TH-PPM or TH-PAM) and transmit with unit power. Each user "sees" an independent channel whose statistics are as described above. The user signals $\{s_k(t)\}_{k=1}^{K_u}$ are asynchronous, meaning that the beginning of a symbol in $s_k(t)$ has no relation with the beginning of a symbol in $s_m(t)$ for $m \neq k$. Henceforth, $s_1(t)$ is viewed as the "desired" signal and its subscript "1" is temporarily dropped to ease the notations. The received waveform is given by

$$r(t) = X \sum_{l=1}^{L} \sum_{k=1}^{K} \alpha_{k,l} s(t - T_l - \tau_{k,l}) + m(t) + n(t) \tag{7}$$

where the double summation represents the useful signal, $m(t)$ accounts for the MAI and $n(t)$ is the thermal noise.

III. Rake Receiver

A. Selective Rake Receiver

The goal of a Rake receiver is to combine the energies of the useful signal components. Unfortunately, as a typical UWB channel has hundreds of resolvable paths, too many "fingers" would be necessary to capture all these energies. In practice, power-consumption and channel-estimation issues limit the number of fingers to ten or so. This prompts the notion of selective Rake (S-Rake) [7], in which only the strongest paths are exploited. By contrast, an all Rake (A-Rake) is an ideal receiver in which all the resolvable paths are combined. Its performance establishes a benchmark for practical receivers. In the sequel, an S-Rake with Q fingers is denoted SQ-Rake.

An S-Rake operates as follows. Call $\{\alpha_q\}_{q=1}^{Q}$ the gains of the Q strongest paths and $\{\tau_q\}_{q=1}^{Q}$ the corresponding delays. Also, assume that the receiver has achieved perfect symbol synchronization for the desired signal. Then, the decision

statistic for symbol a_i is a weighted sum of the type (maximum ratio combiner)

$$x_i = \sum_{q=1}^{Q} \hat{\alpha}_q \int_{iN_fT_f}^{(i+1)N_fT_f} r(t)v(t - iN_fT_f - \hat{\tau}_q)\mathrm{d}t \qquad (8)$$

where $\{\hat{\alpha}_q\}$ and $\{\hat{\tau}_q\}$ are the gain and delay estimates and $v(t)$ is a template waveform depending on the signaling format

$$v(t) = \begin{cases} b(t) - b(t-\Delta), & \text{with TH-PPM} \\ b(t), & \text{with TH-PAM.} \end{cases} \qquad (9)$$

With TH-PPM, a decision $\hat{a}_i = 0$ or 1 is made according to whether x_i is positive or negative.

With TH-PAM, the corresponding decision is $\hat{a}_i = +1$ or -1.

B. Channel Estimation

Channel estimation is performed as indicated in [10]. It is assumed that the monocycle shape is known at the receiver and a training sequence $\{a_i\}$ is transmitted. The goal is to measure the pairs $(\hat{\alpha}_q, \hat{\tau}_q)$ appearing in (8). To this end, a least squares approach is adopted in which the cost function

$$J = \int_0^{T_0} \left[r(t) - \sum_{q=1}^{Q} \tilde{\alpha}_q s(t - \tilde{\tau}_q) \right]^2 \mathrm{d}t \qquad (10)$$

is minimized with respect to the trial values $\{\tilde{\alpha}_q\}$ and $\{\tilde{\tau}_q\}$ of the gains and delays. The observation interval $0 \le t \le T_0$ is taken as a multiple M of the symbol period N_fT_f.

Assume that $s(t - \tilde{\tau}_p)$ and $s(t - \tilde{\tau}_q)$ are approximately orthogonal for $p \neq q$ (due to the extremely narrow width of the monocycles). Then, inserting (1) and (3) into (10) and taking $M \gg 1$, it is found that minimizing J amounts to maximizing the function

$$F = 2\sum_{q=1}^{Q} \tilde{\alpha}_q \int_0^{N_fT_f} R(t, \tilde{\tau}_q)b(t)\mathrm{d}t - B\sum_{q=1}^{Q} \tilde{\alpha}_q^2 \qquad (11)$$

where B is the energy of $b(t)$

$$B = \int_{-\infty}^{+\infty} b^2(t)\mathrm{d}t \qquad (12)$$

and

$$R(t, \tilde{\tau}_q) = \frac{1}{M} \times \begin{cases} \sum_{m=0}^{M-1} r(t + mN_fT_f + a_m\Delta + \tilde{\tau}_q), & \text{for TH-PPM} \\ \sum_{m=0}^{M-1} a_m r(t + mN_fT_f + \tilde{\tau}_q), & \text{for TH-PAM.} \end{cases} \qquad (13)$$

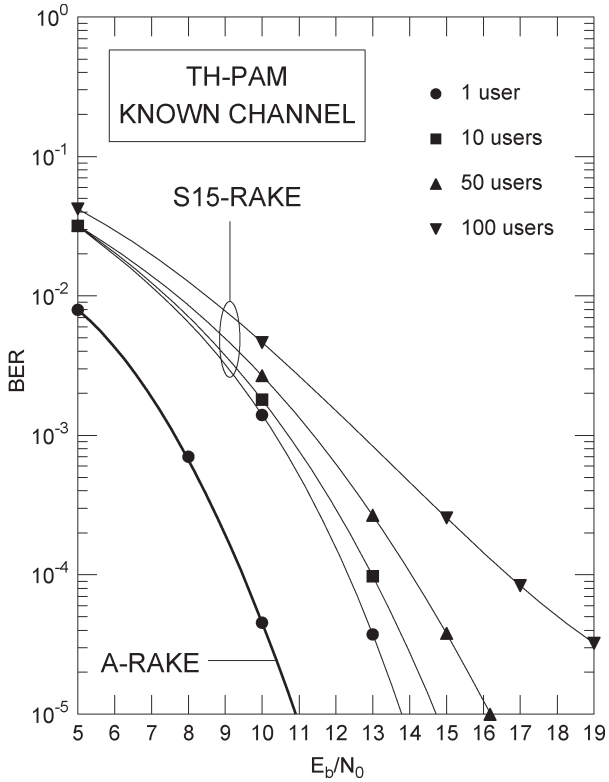

Fig. 1. BER performance with TH-PAM and a known channel.

The maximization is carried out in two steps. First, the delays are kept fixed and the gains are varied until a maximum is reached. This gives the optimal gains as a function of the delays. Next, the gains are plugged into F and the maximum is further looked for with respect to the delays. Skipping the details, it turns out that the delay estimates $\{\hat{\tau}_q\}$ correspond to the Q highest maxima of the function

$$\Phi(\tilde{\tau}) = \left| \int_0^{N_fT_f} R(t, \tilde{\tau})b(t)\mathrm{d}t \right| \qquad (14)$$

while the gain estimates are given by

$$\hat{\alpha}_q = \frac{1}{B} \int_0^{N_fT_f} R(t, \hat{\tau}_q)b(t)\mathrm{d}t \quad 1 \le q \le Q. \qquad (15)$$

IV. Discussion

A. Simulation Results

Simulations have been run to compare the BER performance of Rake receivers with either TH-PPM or TH-PAM signaling. The following values of the signal parameters have been chosen. The monocycle $g(t)$ has a width of 1 ns and the shape of the second derivative of a Gaussian function. The time shift Δ associated with TH-PPM [see (1)] equals 2 ns. A symbol period is made up of 20 frames ($N_f = 20$) and each frame has a duration $T_f = 100$ ns. This corresponds to a bit rate of 500 kbits/s.

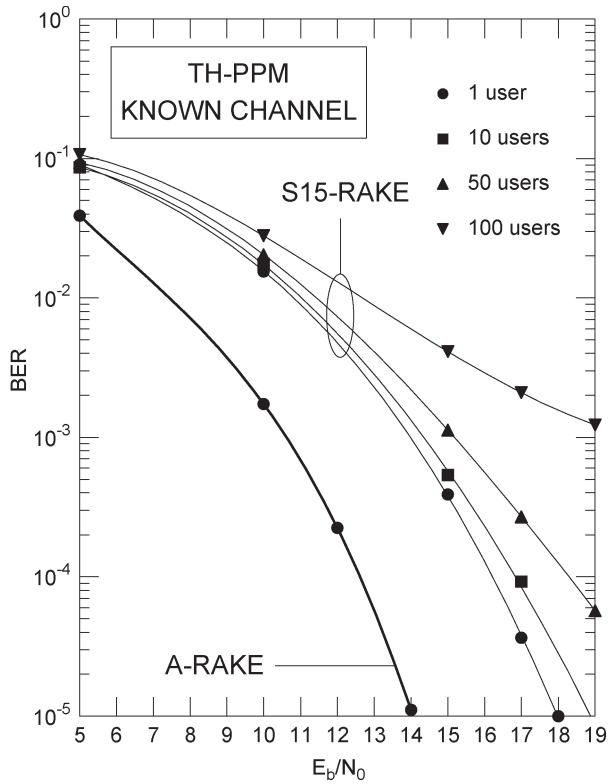

Fig. 2. BER performance with TH-PPM and a known channel.

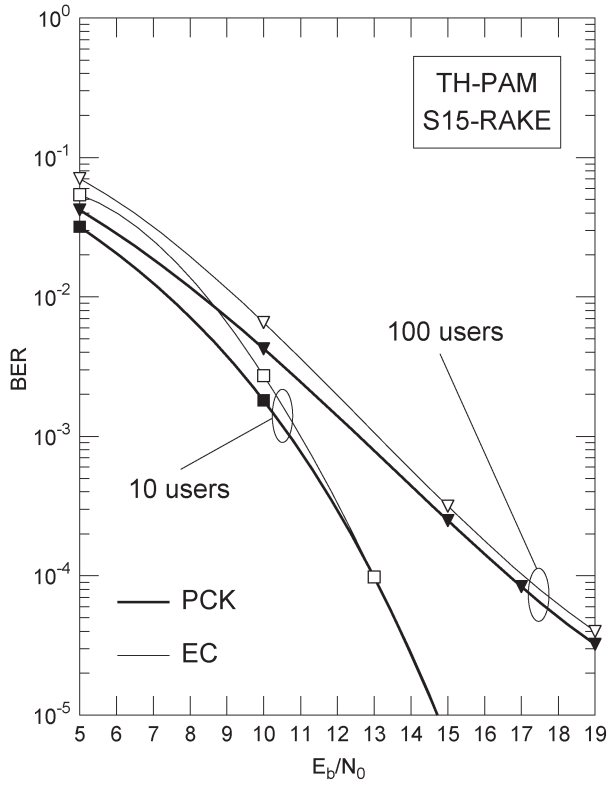

Fig. 3. BER performance with TH-PAM and EC.

For each user, the elements of the time-hopping sequence $\{c_j\}$ are taken randomly from the set $0 \leq c_j \leq 39$ $(N_h = 40)$ and the chip period is $T_c = 1$ ns. Considering that the length of the channel response is about 60 ns, it is realized that the interframe interference is negligible. An observation interval of 50 symbols is used for channel estimation $(M = 50)$.

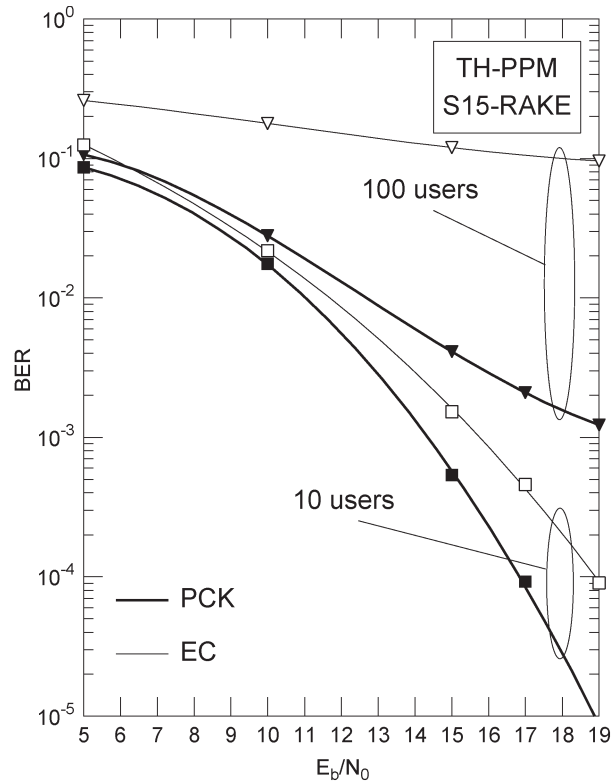

Fig. 4. BER performance with TH-PPM and EC.

Figs. 1 and 2 illustrate the BER curves for an S-Rake with 15 fingers as a function of the ratio E_b/N_0 between the energy per bit and the noise power spectral density. Perfect knowledge of $\{\alpha_q\}$ and $\{\tau_q\}$ is assumed. In each figure, the lower curve corresponds to an A-Rake operating with no MAI (single-user transmission). It turns out (but it is not shown in the figures) that this bound is practically achieved with an S-Rake with 100 fingers. It is seen that the A-Rake with TH-PAM has an edge of 3 dB over the A-Rake with TH-PPM. This is just what we expected since the received signals are (approximately) antipodal with TH-PAM and orthogonal with TH-PPM.

Returning to Figs. 1 and 2, it is seen that, with a single user, the performance degrades by 3 dB in passing from A-Rake to S15-Rake. This seems a tolerable sacrifice in view of the dramatic reduction in complexity and is in keeping with previous results [3] on the robustness of UWB signals. Clearly, the gap from the bound increases with the number of users. It should be noted, however, that the increase is significantly larger with TH-PPM than with TH-PAM.

Figs. 3 and 4 are analogous to Figs. 1 and 2, except that only S15-Rakes are now considered. Thick lines indicate operation with PCK, while thin lines correspond to an estimated channel (EC). The discrepancy between TH-PAM and TH-PPM is striking. With the former, the impact of the estimation errors is limited even with many users [a fraction of a decibel in terms of signal-to-noise ratio (SNR)]. With the latter, vice versa, the degradation is about 2 dB with ten users and becomes huge with 100 users.

B. Interpretation

An obvious question is why TH-PPM is much weaker than TH-PAM as far as MAI is concerned. An intuitive explanation is provided in the following scenario.

1) Propagation occurs in an LOS fashion.
2) The training sequence is the repetition of the same symbol (say $a_i = 1$ with TH-PAM and $a_i = 0$ with TH-PPM).

A more general discussion is possible but its results would be obscured by mathematical details.

Because of assumption 1), the received waveform takes the form

$$r(t) = \sum_{k=1}^{K_u} \alpha^{(k)} s_k\left(t - \tau^{(k)}\right) + n(t) \tag{16}$$

where $\alpha^{(k)}$ and $\tau^{(k)}$ are the attenuation and delay incurred by the kth user's signal. Also, (11) reduces to

$$F = 2\tilde{\alpha}^{(1)} \int_0^{N_f T_f} R\left(t, \tilde{\tau}^{(1)}\right) b(t)\mathrm{d}t - B\tilde{\alpha}^{(1)^2} \tag{17}$$

where $\tilde{\tau}^{(1)}$ is a trial value of $\tau^{(1)}$ and $R(t, \tilde{\tau}^{(1)})$ is given by [see (13)]

$$R\left(t, \tilde{\tau}^{(1)}\right) = \frac{1}{M} \sum_{m=0}^{M-1} r\left(t + mN_f T_f + \tilde{\tau}^{(1)}\right) \tag{18}$$

for both TH-PPM and TH-PAM. In writing (18), assumption 2) has been exploited. Our aim is to compute the contribution to (18) of a single $s_k(t)$ $(k \geq 2)$ when TH-PPM or TH-PAM is used. Loosely speaking, the larger this contribution, say $R^{(k)}(t, \tilde{\tau}^{(1)})$, the stronger is the impact on the estimation accuracy. From (16), it is seen that $R^{(k)}(t, \tilde{\tau}^{(1)})$ is computed by replacing $r(t)$ with $\alpha^{(k)} s_k(t - \tau^{(k)})$ in (18)

$$R^{(k)}\left(t, \tilde{\tau}^{(1)}\right) = \alpha^{(k)} \frac{1}{M} \sum_{m=0}^{M-1} s_k(t + mN_f T_f + \delta_{1,k}) \tag{19}$$

where $\delta_{1,k} = \tilde{\tau}^{(1)} - \tau^{(k)}$.

Let us now specialize (19) for TH-PAM and TH-PPM. In the first case, substituting (3) into (19) yields

$$\frac{R^{(k)}\left(t, \tilde{\tau}^{(1)}\right)}{\alpha^{(k)}} = \sum_j \left[\frac{1}{M} \sum_{m=0}^{M-1} a_{m-j}^{(k)}\right] b(t + jN_f T_f + \delta_{1,k}) \tag{20}$$

where $a_i^{(k)}$ are the kth user's data. In the second case, $s_k(t)$ has the form (1), and (19) becomes

$$\frac{R^{(k)}\left(t, \tilde{\tau}^{(1)}\right)}{\alpha^{(k)}} = \sum_j \left[\frac{1}{M} \sum_{m=0}^{M-1} b\left(t + jN_f T_f - a_{m-j}^{(k)}\Delta + \delta_{1,k}\right)\right]. \tag{21}$$

Bearing in mind that in (21) the data symbols are 0 or 1, it is easily checked that the following identity holds true:

$$b\left(t - a_{m-j}^{(k)}\Delta\right) = a_{m-j}^{(k)} b(t - \Delta) + \left(1 - a_{m-j}^{(k)}\right) b(t) \tag{22}$$

so that (21) may be rearranged as

$$\frac{R^{(k)}\left(t, \tilde{\tau}^{(1)}\right)}{\alpha^{(k)}} = \sum_j \left\{\left[\frac{1}{M} \sum_{m=0}^{M-1} a_{m-j}^{(k)}\right] b(t + jN_f T_f - \Delta + \delta_{1,k}) + \left[\frac{1}{M} \sum_{m=0}^{M-1} \left(1 - a_{m-j}^{(k)}\right)\right] b(t + jN_f T_f + \delta_{1,k})\right\}. \tag{23}$$

For $M \gg 1$, the difference between (20) and (23) is evident. For any index j in (21), there is a $b(t)$-shaped pulse with amplitude much smaller than unity because the symbols $a_{m-j}^{(k)} = \pm 1$ tend to add up in a destructive way. On the contrary, in (23), we have two $b(t)$-shaped pulses with amplitude about 0.5 each. This is so because in a sequence of M symbols, there are, on average, as many ones as zeros. In summary, the impact of MAI is different in two respects: 1) for a given M, it is much larger with TH-PPM than with TH-PAM; 2) as M increases, the impact fades away with TH-PAM while it keeps constant with TH-PPM.

V. Conclusion

We have compared the BER performance of Rake receivers operating with TH-PPM and TH-PAM. The channel model is as reported by the IEEE P802.15 Working Group subcommittee. The receivers are endowed with a channel estimation algorithm based on the least squares criterion. Simulation results show that, even with PCK, the TH-PAM is superior to TH-PPM. The superiority increases when the channel is estimated and becomes substantial in the presence of many users. An intuitive explanation of this fact has been provided.

References

[1] M. Z. Win and R. A. Scholtz, "Ultra-wide bandwidth time hopping spread spectrum impulse radio for wireless multiple access communications," *IEEE Trans. Commun.*, vol. 48, no. 4, pp. 679–691, Apr. 2000.

[2] ——, "Impulse radio: How it works," *IEEE Commun. Lett.*, vol. 2, no. 1, pp. 10–12, Jan. 1998.

[3] ——, "On the robustness of ultra-wide bandwidth signals in dense multipath environments," *IEEE Commun. Lett.*, vol. 2, no. 2, pp. 51–53, Feb. 1998.

[4] ——, "On the energy capture of ultra-wide bandwidth signals in dense multipath environments," *IEEE Commun. Lett.*, vol. 2, no. 9, pp. 245–247, Sep. 1998.

[5] C. J. Le-Martret and G. B. Giannakis, "All digital PAM impulse radio for multiple access through frequency selective multipath," in *Proc. Military Communications Conf. (MILCOM)*, Los Angeles, CA, 2000, pp. 655–659.

[6] N. Boubaker and K. B. Letaief, "Ultra wideband DS-SS for multiple access communications using antipodal signaling," in *Proc. IEEE Int. Conf. Communications (ICC)*, Anchorage, AK, May 2003, pp. 2197–2201.

[7] D. Cassioli, M. Z. Win, F. Vatalaro, and A. F. Molish, "Performance of low-complexity Rake reception in a realistic UWB channel," in *Proc. IEEE Int. Conf. Communications (ICC)*, New York, May 2002, pp. 763–767.
[8] IEEE P802.15_SG3a Working Group for Wireless Personal Area Network, *Channel model sub-committee report final*, Feb. 2003.
[9] R. J.-M. Cramer, R. A. Sholtz, and M. Z. Win, "Evaluation of an ultra-wideband propagation channel," *IEEE Trans. Antennas Propag.*, vol. 50, no. 5, pp. 561–569, May 2002.
[10] V. Lottici, A. N. D'Andrea, and U. Mengali, "Channel estimation for ultra-wideband communications," *IEEE J. Sel. Areas Commun.*, vol. 20, no. 9, pp. 1638–1645, Dec. 2002.
[11] M. Z. Win, "A unified spectral analysis of generalized time-hopping spread spectrum signals in the presence of timing jitter," *IEEE J. Sel. Areas Commun.*, vol. 20, no. 9, pp. 1664–1676, Dec. 2002.

Antonio A. D'Amico received the Dr.Eng. degree in electronic engineering and the Ph.D. degree from the University of Pisa, Pisa, Italy, in 1992 and 1997, respectively.

He is currently a Research Fellow in the Department of Information Engineering, University of Pisa. His research interests are in digital communication theory with emphasis on synchronization algorithms, channel estimation, and detection techniques.

Umberto Mengali (M'69–SM'85–F'90) received the degree in electrical engineering from the University of Pisa, Pisa, Italy, and the Libera Docenza degree in telecommunications from the Italian Education Ministry, Italy.

Since 1963, he has been with the Department of Information Engineering, University of Pisa, where he is a Professor of Telecommunications. In 1994, he was a Visiting Professor at the University of Canterbury, New Zealand, as an Erskine Fellow. His research interests are in digital communications and communication theory with emphasis on synchronization methods and modulation techniques. He coauthored the book *Synchronization Techniques for Digital Receivers* (Plenum Press, 1997).

Prof. Mengali is a member of the Communication Theory Committee and was an Editor of the IEEE TRANSACTIONS ON COMMUNICATIONS from 1985 to 1991 and of the *European Transactions on Telecommunications* from 1997 to 2000. He has served on the technical program committees of several international conferences and was the technical Co-Chair of the 2004 International Symposium on Information Theory and Applications (ISITA).

Lorenzo Taponecco was born in Sarzana, Italy, in 1977. He received the Dr.Ing. (*cum laude*) degree in telecommunications engineering from the University of Pisa, Pisa, Italy, in 2002, where he is currently working toward the Ph.D. degree.

Since 2003, he has been with the Department of Information Engineering, University of Pisa. His research interests include digital communication theory with special emphasis on ultrawideband (UWB) communications, parameter estimation, and synchronization techniques.